Bioorganic Chemistry 90 (2019) 103099

Contents lists available at ScienceDirect

Bioorganic Chemistry

journal homepage: www.elsevier.com/locate/bioorg

(±)-Meliviticines A and B: Rearranged prenylated acetophenone derivatives from *Melicope viticina* and their antimicrobial activity

Wei Li[a,b], Li Rao[a], Yu Liu[a], Qian He[a], Yue Fan[a], Yun-Xia You[a], Yu Su[a], Feng Hu[a], You-Kai Xu[c], Bin Lin[d], Sheng Yin[b], Chuan-Rui Zhang[a,*]

[a] Chongqing Key Laboratory of Natural Product Synthesis and Drug Research, and Chemical Biology Research Center, School of Pharmaceutical Sciences, Chongqing University, Chongqing 401331, PR China
[b] School of Pharmaceutical Sciences, Sun Yat-sen University, Guangzhou, Guangdong 510006, PR China
[c] Key Laboratory of Tropical Plant Resource and Sustainable Use, Xishuangbanna Tropical Botanical Garden, Chinese Academy of Sciences, Menglun, Yunnan 666303, PR China
[d] School of Pharmaceutical Engineering, Shenyang Pharmaceutical University, Shenyang 110016, PR China

ARTICLE INFO

Keywords:
Melicope viticina
Prenylated acetophenone derivatives
Absolute configuration
Antimicrobial activity

ABSTRACT

Two new prenylated acetophenone derivatives racemates, meliviticines A (**1**) and B (**2**) with unprecedented rearranged skeletons, were isolated from *Melicope viticina*. Subsequent chiral resolution led to the separation of two pairs of enantiomers, (±)-meliviticines A (**1a**/**1b**) and (±)-meliviticines B (**2a**/**2b**). Their structures including absolute configurations were elucidated by extensive spectroscopic data, electronic circular dichroism analysis, and X-ray crystallography. A plausible biosynthetic pathway of **1** and **2**, involving ring cleavage and rearrangement of the prenylated acetophenone backbone was proposed. All the isolates showed moderate antimicrobial activities with MIC values of 25–50 μg/mL against several bacterial and fungal strains.

1. Introduction

The genus of *Melicope* (Rutaceae) contains about 233 species mainly distributed in the tropical regions of the Eastern Hemisphere [1]. Many species have been used as traditional medicines with diverse pharmacological activities [2–11]. *Melicope* genus is well-known as a rich source of structurally diverse natural products such as alkaloids, flavonoids, benzopyrans, and acetophenones with a wide range of biological activities including antioxidant, antiinflammatory, antipyretic, analgesic, PTP1B inhibitory, neuraminidase inhibitory, antidiabetes, antimalarial, antifungal, and cytotoxic activities [2–18]. Amongst, prenylated acetophenones with skeletal structure of an acetophenone connected with one or more prenyl or geranyl groups, are considered as the most important chemotaxonomic markers of *Melicope* and *Acronychia* species [18–22]. Although there have been a large number of prenylated acetophenones isolated [4–6,9–11,14–17,20–22], only a few showed dearomatized ring [11,15,16,18].

Melicope viticina (Wallich ex Kurz) T. G. Hartley, a deciduous shrub or tree distributed in Yunnan province, China and Southeast Asia, has never been studied before. To search for more bioactive metabolites from plants, two rearranged nonaromatic prenylated acetophenone derivatives, meliviticines A (**1**) and B (**2**) with unprecedented dearomatic skeletons were isolated from the leaves and twigs of *M. viticina* in this study (see Fig. 1). Further chiral-phase separation led to two pairs of enantiomers, (±)-meliviticines A (**1a**/**1b**) and (±)-meliviticines B (**2a**/**2b**). The antimicrobial activity was evaluated against a panel of bacteria and fungi, and the results showed all the isolates with moderate activities. Herein the isolation, structural elucidation, plausible biosynthetic formation and antimicrobial activity were presented.

2. Materials and methods

2.1. General experimental procedures

Optical rotations were measured with a Rudolph Autopol I automatic polarimeter. UV spectra were recorded on a Shimadzu UV-2450 spectrophotometer and CD spectra on an Applied Photophysics Chirascan spectrometer. IR spectra were recorded on a Bruker Tensor 37 infrared spectrometer using KBr disks. NMR spectra were recorded with a Bruker AM-400 instrument. HRESIMS were recorded on a Waters Micromass Q-TOF spectrometer. Semipreparative HPLC was performed on a Shimadzu LC-20 AT and an SPD-M20A PDA detector with a YMC-pack ODS-A column (10 × 250 mm, S-5 μm, 12 nm) and a chiral column (Phenomenex Lux, cellulose-2, 10 × 250 mm, 5 μm). Column

* Corresponding author.
E-mail address: crzhang@cqu.edu.cn (C.-R. Zhang).

https://doi.org/10.1016/j.bioorg.2019.103099
Received 27 April 2019; Received in revised form 27 June 2019; Accepted 28 June 2019
Available online 03 July 2019

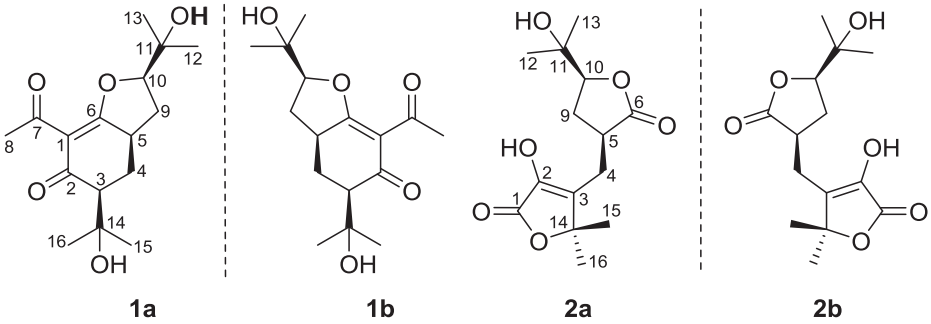

Fig. 1. Structures of compounds **1** and **2**.

Table 1
^{1}H and ^{13}C NMR Data of **1** and **2** (δ in ppm and J values in Hz).

No.	1				2	
	δ_C[a]	δ_H[a]	δ_C[b]	δ_H[b]	δ_C[a]	δ_H[a]
1	115.0		114.4		169.3	
2	200.3		199.2		137.4	
3	54.6	2.40 (m)	54.5	2.35 (m)	135.3	
4a	29.3	2.30 (m)	28.5	2.30 (m)	25.7	2.78 (dd, 16.4, 3.3)
4b		1.48 (dd, 12.6, 12.6)		1.41 (dd, 12.3, 12.3)		2.31 (dd, 16.4, 10.1)
5	41.9	3.11 (m)	40.8	3.24 (m)	38.7	3.28 (m)
6	183.7		183.6		178.4	
7	198.1		196.4			
8	32.0	2.38 (s)	31.7	2.22 (s)		
9a	29.8	2.28 (m)	29.4	2.27 (m)	29.5	2.42 (m)
9b		1.86 (dd, 11.7, 11.7)		1.69 (dd, 11.8, 11.8)		1.94 (dd, 11.5, 11.5)
10	94.4	4.54 (dd, 10.9, 5.2)	94.1	4.56 (dd, 10.9, 5.3)	84.4	4.26 (dd, 10.0, 6.0)
11	69.9		68.9		70.3	
12	24.5	1.16 (s)	25.7[c]	1.08 (s)[c]	24.0	1.15 (s)
13	26.9	1.37 (s)	26.1[c]	1.19 (s)[c]	26.6	1.32 (s)
14	72.9		71.8		84.7	
15	24.5[c]	1.20 (s)	26.8[c]	1.22 (s)[c]	25.3[c]	1.42 (s)
16	28.5[c]	1.20 (s)	27.5[c]	1.07 (s)[c]	25.2[c]	1.42 (s)
OH				11-OH 4.74 (s) 14-OH 5.05 (s)		

[a] Measured in $CDCl_3$ for ^{1}H (400 MHz) and ^{13}C (100 MHz).
[b] Measured in DMSO-d_6 for ^{1}H (500 MHz) and ^{13}C (125 MHz).
[c] Exchangeable.

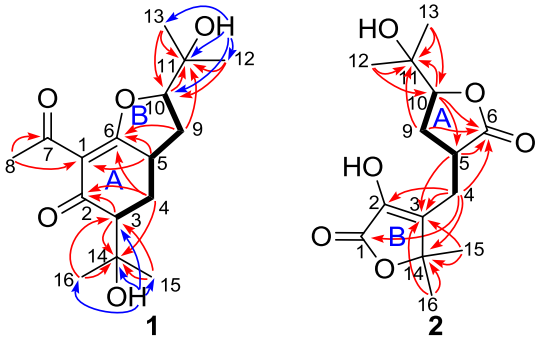

Fig. 2. $^{1}H-^{1}H$ COSY (▬) and HMBC (→ measured in $CDCl_3$; → measured in DMSO-d_6) correlations of **1** and **2**.

chromatography (CC) was performed on silica gel (200–300 mesh, Qingdao Haiyang Chemical Co., Ltd.), MCI gel (CHP20P, 75–150 μm, Mitsubishi Chemical Industries Ltd.) and reversed-phase (RP) silica gel C18 (12 nm, S-5 μm, YMC Co., Ltd.). Thin-layer chromatography (TLC) was performed on silica gel 60 GF254 plates (Qingdao Haiyang Chemical Co., Ltd.). All solvent used were obtained from ChengDu Chron Chemicals Co., Ltd.

2.2. Plant material

The leaves and twigs of *Melicope viticina* were collected from Xishuangbanna Tropical Botanical Garden, Yunnan Province, China, in August 2017 and identified by Professor You-Kai Xu of Xishuangbanna Tropical Botanical Garden, Chinese Academy of Sciences. A voucher specimen has been deposited in School of Pharmaceutical Sciences, Chongqing University (Accession number CRZ2017MV).

2.3. Extraction and isolation

The air-dried and powdered leaves and twigs (10.2 kg) of *M. viticina* was extracted with 95% ethanol (3 × 50 L) at room temperature and evaporation of solvent under reduced pressure afforded a crude extract (450 g), which was then suspended in H_2O (1.5 L) and sequentially partitioned with petroleum ether (4 × 1 L), EtOAc (4 × 1 L) and *n*-BuOH (4 × 1 L). After the evaporation of solvent, the EtOAc fraction (150 g) was chromatographed on a MCI gel column eluted with MeOH-H_2O (3:7–10:0) in gradient to yield five fractions. Fraction 1 (38.9 g) was subjected to a silica gel CC eluted with $CHCl_3$-MeOH (100:1–10:1) to give five fractions F1a–F1e. A portion (1.0 g) of F1c (3.6 g) was fractionated on a silica gel CC eluted with petrol-EtOAc (3:1–1:3) to get four fractions F1c1–F1c4. F1c1 (110 mg) was separated on an RP-18 CC eluted with MeOH-H_2O (40:60) and then purified by semi-preparative HPLC with MeCN-H_2O (30:70, 3 mL/min) to give **1** (27 mg, t_R 12 min). Similarly, F1c2 (180 mg) was separated on an RP-18 CC eluted with MeOH-H_2O (30:70) and then purified by semi-preparative HPLC with MeCN-H_2O (20:80, 3 mL/min) to give **2** (30 mg, t_R 12 min). The resolution of racemic mixture **1** and **2** was performed by HPLC equipped with a chiral-phase column (MeCN/H_2O, 35:65 and 30:70, 3 mL/min) to give **1b** (8.0 mg, t_R 10.3 min) and **1a** (9.0 mg, t_R 10.8 min), and **2a** (10.0 mg, t_R 9.0 min) and **2b** (11.4 mg, t_R 9.5 min), respectively.

2.4. Spectroscopic data

Meliviticines A (**1**): Colorless amorphous solid; UV (MeOH) λ_{max} (log ε) 260 (4.15) nm; IR (KBr) ν_{max} 3000–3700 (br), 2976, 1754, 1674, 1618, 1593, 1466, 1379, 1301, 1266, 1240, 1207, 1175, 1040, 942, 847 cm^{-1}; for ^{1}H and ^{13}C NMR data, see Table 1; HRESIMS *m/z* 297.1685 $[M+H]^+$ (calcd for $C_{16}H_{25}O_5$, 297.1697); **1a**: $[\alpha]_D^{25}$ +48.4 (*c* 3.33, MeCN); CD (MeCN): $\Delta\varepsilon$ (λ_{230}) −5.05, (λ_{267}) −5.08, (λ_{310}) +5.91; **1b**: $[\alpha]_D^{25}$ −50.1 (*c* 1.67, MeCN); CD (MeCN): $\Delta\varepsilon$ (λ_{231}) +5.77, (λ_{266}) +5.71, (λ_{310}) −5.86.

Meliviticines B (**2**): Colorless amorphous solid; UV (MeOH) λ_{max} (log ε) 231 (4.05) nm; IR (KBr) ν_{max} 3000–3700 (br), 2980, 1739, 1461, 1368, 1227, 1186, 1111, 1037 cm^{-1}; for ^{1}H and ^{13}C NMR data, see Table 1; HRESIMS *m/z* 285.1321 $[M+H]^+$ (calcd for $C_{14}H_{21}O_6$, 285.1333); **2a**: colorless crystals (petroleum ether/EtOAc, 8:1), mp

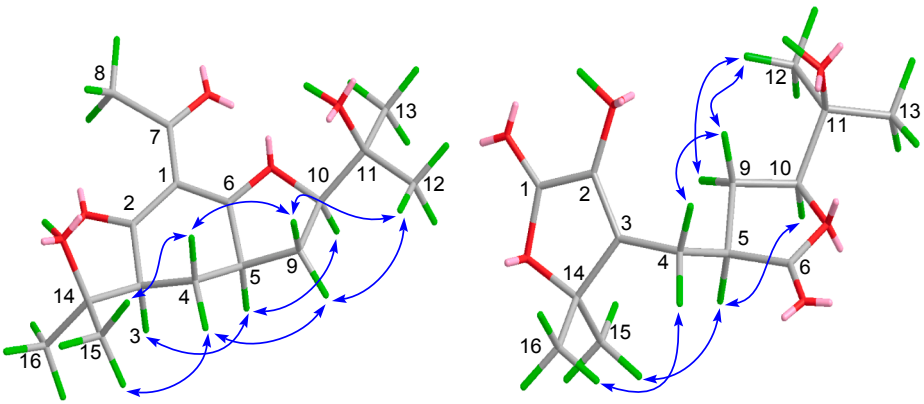

Fig. 3. Key NOESY correlations (^{1}H ↔ ^{1}H) of **1** (left) and **2** (right).

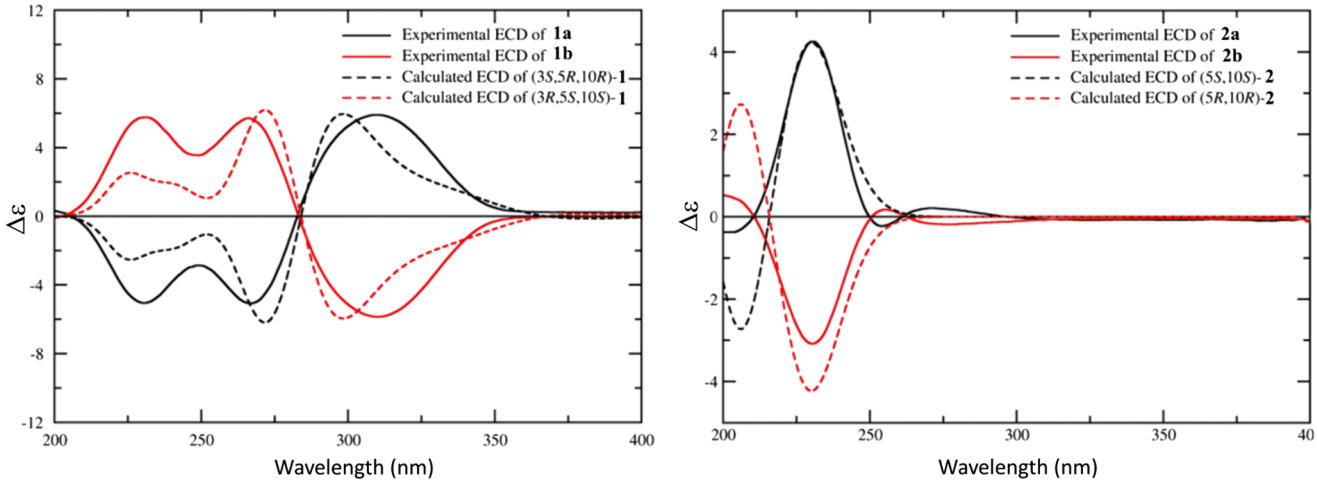

Fig. 4. Experimental and calculated ECD spectra of **1** and **2**.

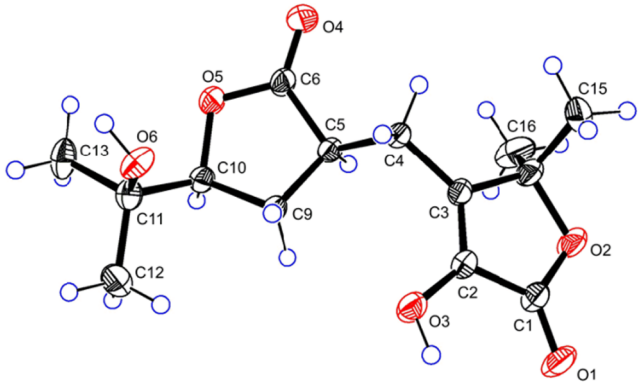

Fig. 5. ORTEP diagram of **2a**.

142–144 °C; $[\alpha]_D^{25}$ +66.4 (*c* 2.50, MeCN); CD (MeCN): $\Delta\varepsilon$ (λ_{231}) +4.25; **2b**: $[\alpha]_D^{25}$ −58.0 (*c* 3.13, MeCN); CD (MeCN): $\Delta\varepsilon$ (λ_{230}) −3.08.

2.5. X-ray crystal structure analysis

Single crystal of **2a** was collected on an Xcalibur, Onyx, Nova diffractometer equipped with Cu K α radiation (λ = 1.54184 Å). The structure was determined using direct methods and refined using olex2. All non-hydrogen atoms were refined using anisotropic thermal parameters. Hydrogen atoms were located by geometrical calculations. The absolute configuration was confirmed by refinement of the Flack parameters. Crystallographic data have been deposited at the Cambridge Crystallographic Data Centre, CCDC Number 1903989 (**2a**). These data are available free of charge from The Cambridge Crystallographic Data Centre via www.ccdc.cam.ac.uk/data_request/cif.

Crystal data for (+) meliviticines B (**2a**). $C_{14}H_{20}O_6$ (M = 284.30 g/mol): monoclinic, space group $C2$ (no. 5), a = 23.2522(4) Å, b = 5.84900(10) Å, c = 10.83349(19) Å, β = 99.6403(16)°, V = 1452.57(4) Å^3, Z = 4, T = 100 K, μ(Cu Kα) = 0.852 mm^{-1}, $Dcalc$ = 1.300 g/cm^3, 13,691 reflections measured (7.714° ≤ 2Θ ≤ 144.21°), 2849 unique (R_{int} = 0.0304, R_{sigma} = 0.0197) which were used in all calculations. The final R_1 was 0.0284 (I > 2σ(I)) and wR_2 was 0.0733 (all data). Flack parameter = 0.08 (6).

2.6. Antimicrobial assays

Antimicrobial assays were conducted as described previously [23–25]. All the isolates were evaluated for antibacterial activity against *Micrococcus lysodeikticus*, *Bacillus megaterium*, *Bacterium paratyphosum B*, Methicillin-resistant *Staphylococcus aureu*, *Salmonella typhi*, *Pseudomonas aeruginosa* strains and antifungal activity against *Verticillium dahliae* Kleb, *Alternaria alternate*, *Rhizoctonia solani*, *Sclerotinia sclerotiorun*, *Phytophthora parasitica*, *Gibberella saubinetii* strains.

3. Results and discussion

Meliviticine A (**1**) possessed a molecular formula of $C_{16}H_{24}O_5$ as determined by the HRESIMS m/z 297.1685 $[M+H]^+$ (calcd for $C_{16}H_{25}O_5$, 297.1697), corresponding to 5° of unsaturation (DOUs). The IR spectrum absorption bands at 3397, 1673, and 1617 cm^{-1} indicated

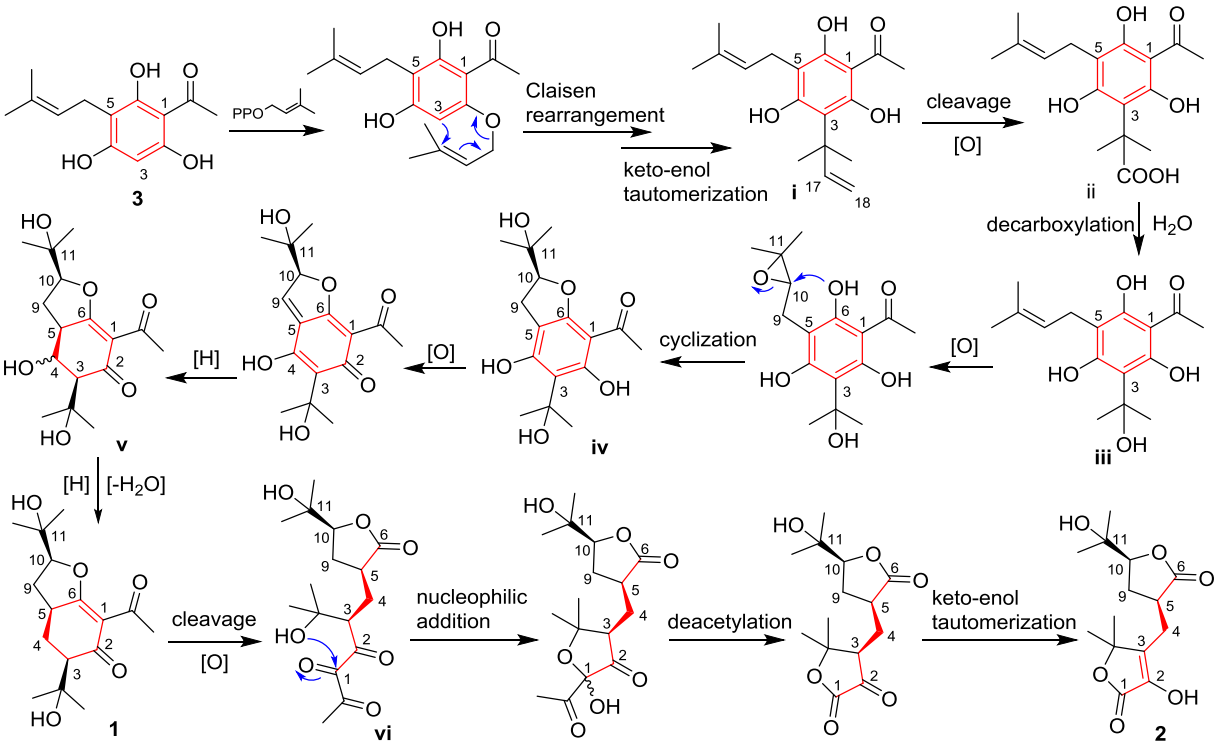

Scheme 1. Putative Biosynthetic Pathway toward the Formation of **1** and **2**.

Table 2
Antibacterial activity of the isolates (MIC, μg/mL).

Strain	Compounds				Positive control
	1a	**1b**	**2a**	**2b**	Ciprofloxacin
Micrococcus lysodeikticus	50.0	50.0	50.0	50.0	0.8
Bacillus subtilis	50.0	50.0	50.0	50.0	0.8
Bacterium paratyphosum B	25.0	25.0	25.0	25.0	0.8
Methicillin-resistant *Staphylococcus aureus*	50.0	50.0	50.0	50.0	0.8
Salmonella typhi	50.0	50.0	50.0	50.0	0.8
Pseudomonas aeruginosa	50.0	50.0	50.0	50.0	0.8

Table 3
Antifungal activity of the isolates (MIC, μg/mL).

strain	Compounds				Positive control
	1a	**1b**	**2a**	**2b**	Ketoconazole
Verticillium dahliae Kleb	50.0	50.0	50.0	50.0	3.1
Alternaria alternata	25.0	25.0	25.0	25.0	3.1
Rhizoctonia solani	100.0	100.0	100.0	100.0	3.1
Sclerotinia sclerotiorum	100.0	100.0	100.0	100.0	1.6
Phytophthora parasitica	25.0	25.0	25.0	25.0	3.1
Gibberella saubinetii	50.0	50.0	50.0	50.0	1.6

the presence of hydroxyl, carbonyl, and vinyl groups, respectively. The ^{1}H NMR spectrum (Table 1) displayed signals for five tertiary methyl protons [δ_H 1.16, 1.37, 2.38 (each 3H, s), and 1.20 (3H × 2, s)], one oxymethine [δ_H 4.54 (1H, dd, J = 10.9, 5.2 Hz)], and six aliphatic protons. The ^{13}C NMR spectrum (Table 1) with the help of DEPT experiments and HSQC spectrum resolved 16 carbons into the categories two ketocarbonyl groups (δ_C 198.1 and 200.3), one oxygenated double bond (δ_C 115.0 and 183.7), five methyls, two sp^3 methylenes, three sp^3 methines (one oxygenated at δ_C 94.4), two oxygenated sp^3 quaternary carbons (δ_C 72.9 and 69.9), accounting for three of the five DOUs, which suggested that **1** was bicyclic. The planar structure of **1** was elucidated by analysis of the 2D NMR data (Fig. 2). The fragment of oxygenated methine CH-10 and six aliphatic protons CH_2-CH-CH_2-CH was established as shown in Fig. 2 by the $^1H-^1H$ COSY correlations of H-3/H_2-4, H_2-4/H-5, H-5/H_2-9, and H_2-9/H-10. The HMBC correlations of H-3/C-2, H-4/C-2 and C-6, H-5/C-1 and C-6 together with the $^1H-^1H$ COSY correlations of H-3/H_2-4 and H_2-4/H-5 confirmed the connection of C-2–C-3–C-4–C-5–C-6–C-1. One oxygenated isopropyl group was connected to C-3 by the HMBC correlations from Me-15 and Me-16 to C-3 and one oxygenated sp^3 quaternary carbon C-14 (δ_C 72.9). Another oxygenated isopropyl group was connected to C-10 by the HMBC correlations from Me-12 and Me-13 to C-10 and another sp^3 oxygenated quaternary carbon C-11 (δ_C 69.9). Besides, one acetyl group was attached to C-1 by the HMBC correlations of Me-8/C-1 and C-7. Unfortunately, two hydroxyl groups could not be assigned due to the absence of their proton resonances when tested in $CDCl_3$. The connections of C-1 to C-2 and C-6 to C-10 could not be determined either since there were no any useful HMBC correlations observed. To resolve those assignments, the ^{1}H, ^{13}C, HSQC and HMBC spectra of **1** were tested again in DMSO-d_6. Two hydroxyl groups were then attached to C-11 and C-14 as two dimethylcarbinol groups by the HMBC correlations from 11-OH to C-10, C-11, C-12 and C-13, and from 14-OH to C-3, C-14, C-15 and C-16, respectively (Fig. 2). Thus, we could connect the oxygenated methine C-10 (δ_C 94.4) to C-6 (δ_C 183.7) belonging to the oxygenated double bond C-6/C-1 through the ether bond to form a typical furanoid ring (ring B), and then the α,β-unsaturated ketone group was determined to connect C-1 and C-2 to form the ring A as a cyclohexenone moiety by the chemical shift of C-2 (δ_C 200.3) and C-7 (δ_C 198.1), which showed the presence of conjugated ketone carbonyl groups. The above analysis was also in accord with the bicyclic structure of **1**. Therefore, the gross structure of **1** was established as a nonaromatic prenylated and isopropylated acetophenone derivative.

The relative stereochemistry of **1** was determined by the NOESY experiment (Fig. 3), where the correlations of H-5/H-3 and H-10 suggested they were cofacial, which was also supported by the NOESY correlations of H_2-4/Me-15, H-4a/H-9a, H-4b/H-9b and H_2-9/Me-12.

The specific optical rotation value of **1** was almost zero, which

suggested that it could be a racemic mixture. Subsequent chiral HPLC resolution was performed to yield a pair of enantiomers, **1a** and **1b**, which exhibited opposite optical rotation and electronic circular dichroism (ECD). To elucidate the absolute configurations of them, the theoretical ECD spectra were calculated using the time-dependent density functional theory (TDDFT) at the B3LYP/6–311 + + G(2d,p) level with MeCN as the solvent in the Conductor-like Polarizable Continuum Model (CPCM) [26–28]. The calculated and experimental ECD spectra matched well, which assigned the absolute configurations of **1a** and **1b** as 3*S*, 5*R*, 10*R* and 3*R*, 5*S*, 10*S*, respectively (Fig. 4).

Meliviticine B (**2**) had the molecular formula of $C_{14}H_{20}O_6$ based on the HRESIMS *m/z* 285.1321 $[M+H]^+$ (calcd for $C_{14}H_{21}O_6$, 285.1333), corresponding to 5 DOUs. The ^{1}H NMR spectrum (Table 1) displayed signals for four tertiary methyl protons [δ_H 1.15, 1.32 (each 3H, s), and 1.42 (3H × 2, s)], one oxymethine [δ_H 4.26 (1H, dd, J = 10.0, 6.0 Hz)], and five aliphatic protons. The ^{13}C NMR together with DEPT and HSQC spectra (Table 1) resolved 14 carbons, including two ester carbonyls (δ_C 178.4 and 169.3), one double bond (δ_C 137.4 and 135.3), four methyls, two sp^3 methylenes, two sp^3 methines (one oxygenated at δ_C 84.4), two oxygenated sp^3 qua ternary carbons (δ_C 84.7 and 70.3), accounting for three of the five DOUs. Therefore **2** was also bicyclic. The planar structure of **2** was established by the 2D NMR spectra (Fig. 2). The fragment of oxygenated methine CH-10 and five aliphatic protons CH_2-CH-CH_2 was established as displayed in Fig. 2 by the ^{1}H − ^{1}H COSY correlations of H_2-4/H-5, H-5/H_2-9 and H_2-9/H-10. Then the HMBC correlations from H_2-4, H-5, H_2-9 and H-10 to C-6 completed the assignment of a five-membered lactone (ring A). Comparing with the NMR data of **1**, one dimethylcarbinol group was determined and connected to C-10 by the HMBC correlations from Me-12 and Me-13 to C-10 and one sp^3 oxygenated quaternary carbon C-11 (δ_C 70.3). The HMBC correlations of H_2-4/C-1, C-2 and C-3, and H-5/C-3 assigned the connection of C-1–C-2–C-3–C-4–C-5. One oxygenated isopropyl group was connected to C-3 by the HMBC correlations from Me-15 and Me-16 to C-3 and one oxygenated sp^3 quaternary carbon C-14 (δ_C 84.7). Although the connection of two quaternary carbon C-1 and C-14 could not be determined directly by the 2D NMR spectra, we still temporally assigned the ring B as another five-membered lactone (ring B) by the chemical shift of C-1 (δ_C 169.3) and C-14. Lastly, one hydroxyl group had to be attached to C-2, which was supported by the chemical shifts of C-2 (δ_C 137.4) and C-3 (δ_C 135.3). Thus **2** was established as a rearranged prenylated and isopropylated acetophenone derivative with aromatic ring cleavage and acetyl group decomposition.

The relative configuration of **2** was determined by analysis of the NOESY spectrum (Fig. 3). The important NOESY correlation of H-10/H-5 suggested they were cofacial, which was also supported by the NOESY correlations of H-4a/Me-15, H-5/Me-16, H-9b/H-4b and H_2-9/Me-12.

Similarly, the small specific optical rotation value of **2** led to the subsequent chiral HPLC resolution to yield a pair of enantiomers, **2a** and **2b**. Fortunately, we succeeded to acquire crystals of **2a**, and a Cu Kα X-ray crystallography study was then performed, which not only confirmed the planar structure and the relative configuration of **2** but also determined the absolute configuration of **2a** as 5*S* and 10*S* by Flack absolute structure parameter [0.08 (6)] [29] (Fig. 5). Furthermore, the theoretical ECD spectra was calculated and matched well with the experimental ECD spectra, which supported the absolute configurations of **2a** and **2b** as 5*S*, 10*S* and 5*R*, 10*R*, respectively (Fig. 4).

To the best of our knowledge, all the prenylated acetophenones reported so far in the literature represented structurally an acetophenone connected with one or more prenyl or geranyl groups. Meliviticine A (**1**) was the first isopropylated prenylated acetophenone derivatives, while meliviticine B (**2**) represented the first example of the aromatic ring opened as linear and the acetyl group removal from the acetophenone structure. Therefore, the plausible biosynthetic pathway towards the formation of **1** and **2** was proposed as follows (Scheme 1). 2,4,6-trihydroxy-3-prenylacetophenone (**3**) [30], an abundant component occurring in *Melicope* genus, was considered as the precursor. Prenylation of the precursor at 2-OH followed by claisen rearrangement and keto-enol tautomerization afforded intermediate **i**. The cleavage of the C-17–C-18 double bond of **i** accompanied by oxidation of the formyl group to afford **ii**. Decarboxylation of **ii** generated **iii**, which further underwent nonface-selective oxidation and subsequent cyclization would generate **iv** with two possible stereoisomers (*S*, *R*). Then **iv** underwent oxidation and selective reduction generated **v**, which was followed by dehydration and selective reduction to form **1**. Then the vinyl group in **1** was cleaved by oxidation to afford **vi**, which further underwent intramolecular hemiacetal formation and deacetylation followed by keto-enol tautomerization to generate **2**.

1a/**1b** and **2a**/**2b** were tested for antimicrobial activities against six bacterial and six fungal strains, and the results showed all of them with moderate activities with MIC values of 25 μg/mL against one bacteria, *Bacterium paratyphosum* B, and two fungi, *Alternaria alternate* and *Phytophthora parasitica*, comparing with the positive controls with MIC values of 0.8–3.1 μg/mL (Tables 2 and 3). Furthermore, all the isolates showed activities with MIC values of 50 μg/mL against the other five bacteria, *Micrococcus lysodeikticus*, *Bacillus subtilis*, Methicillin-resistant *Staphylococcus aureus*, *Salmonella typhi* and *Pseudomonas aeruginosa*, and two fungi, *Verticillium dahliae* Kleb and *Gibberella saubinetii*, while for the other two fungi, *Rhizoctonia solani* and *Sclerotinia sclerotiorum*, **1a**/**1b** and **2a**/**2b** showed weak activities with MIC values of 100 μg/mL.

Acknowledgements

This work was supported by Chongqing Research and Frontier Technology (cstc2018jcyjAX0517), Fundamental Research Funds for the Central Universities in China (Project No. 106112017CDJXFLX0014 and 106112017CDJQJ468824) and Venture & Innovation Support Program for Chongqing Overseas Returnees (cx2018022). C.-R. Z. is a scholar of “the 100 Talents Project” of Chongqing University.

Appendix A. Supplementary material

Supplementary data to this article can be found online at https://doi.org/10.1016/j.bioorg.2019.103099.

References

[1] D.X. Zhang, T.G. Hartley, Flora of China vol. 11, (2008) 70–73.
[2] I.S. Chen, H.F. Chen, M.J. Cheng, Y.L. Chang, C.M. Teng, I. Tsutomu, J.J. Chen, I.L. Tsai, J. Nat. Prod. 64 (2001) 1143–1147.
[3] H.T. Simonsen, A. Adsersen, P. Bremner, M. Heinrich, U.W. Smitt, J.W. Jaroszewski, Phytother. Res. 18 (2004) 542–545.
[4] J.J. Chen, J.Y. Cho, T.L. Hwang, I.S.J. Chen, J. Nat. Prod. 71 (2008) 71–75.
[5] A.J. Johnson, R.A. Kumar, S.A. Rasheed, S.P. Chandrika, A. Chandrasekhar, S. Baby, A. Subramoniam, J. Ethnopharmacol. 130 (2010) 267–271.
[6] K. Shaari, V. Suppaiah, L.K. Wai, J. Stanslas, B.A. Tejo, D.A. Israf, F. Abas, I.S. Ismail, N.H. Shuaib, S. Zareen, N.H. Lajis, Bioorg. Med. Chem. 19 (2011) 6340–6347.
[7] K. Nakashima, M. Oyama, T. Ito, Y. Akao, J.R. Witono, D. Darnaedi, T. Tanaka, J. Murata, M. Iinuma, Tetrahedron 68 (2012) 2421–2428.
[8] S. George, S.A. Nair, A.J. Johnson, R. Venkataraman, S.J. Baby, Ethnopharmacol. 168 (2015) 158–163.
[9] N.H. Nguyen, T.K.Q. Ha, S. Choi, S. Eum, C.H. Lee, T.T. Bach, V.T. Chinh, W.K. Oh, Phytochemistry 130 (2016) 291–300.
[10] J. Xu, X. Sun, X. Liu, M. Peng, S. Li, D.Q. Jin, D. Lee, M. Bartlam, Y. Guo, J. Funct. Foods 23 (2016) 565–572.
[11] Q.Q. Xu, X.L. Chen, J.F. Xu, S.B. Wang, J.G. Luo, L.Y. Kong, Fitoterapia 132 (2019) 40–45.
[12] F. Tillequin, G. Baudouin, M. Ternoir, M. Koch, J. Pusset, T. Sevenet, J. Nat. Prod. 45 (1982) 486–488.
[13] A.L. Skaltsounis, F. Tillequin, M. Koch, T. Sevenet, J. Nat. Prod. 46 (1983) 732–735.
[14] J.A. Chan, E.A. Shultis, S.A. Carr, C.W. DeBrosse, D.S. Eggleston, T.A. Francis, L.J. Hyland, W.P. Johnson, L.B. Killmer, D.B. Staiger, J.W. Westley, J. Org. Chem. 54 (1989) 2098–2103.
[15] H.T. Simonsen, Phytochem. Lett. 5 (2012) 371–375.
[16] J.F. Xu, H.J. Zhao, X.B. Wang, Z.R. Li, J. Luo, M.H. Yang, L. Yang, W.Y. Yu, H.Q. Yao, J.G. Luo, L.Y. Kong, Org. Lett. 17 (2015) 146–149.
[17] K. Nakashima, N. Abe, F.R. Chang, M. Inoue, M. Oyama, J. Nat. Med. 71 (2017) 299–304.
[18] J.-F. Xu, C. Han, Q.-Q. Xu, X.-B. Wang, H.-J. Zhao, G.-M. Xue, J.-G. Luo, L.-Y. Kong,

J. Nat. Prod. 82 (2019), https://doi.org/10.1021/acs.jnatprod.8b00003.
[19] A. Adsersen, U.W. Smitt, H.T. Simonsen, S.B. Christensen, J.W. Jaroszewski, Biochem. Syst. Ecol. 35 (2007) 447–453.
[20] E. Kouloura, M. Halabalaki, M.C. Lallemand, S. Nam, R. Jove, M. Litaudon, K. Awang, H.A. Hadi, A.L. Skaltsounis, J. Nat. Prod. 75 (2012) 1270–1276.
[21] K. Miyake, A. Suzuki, C. Morita, M. Goto, D.J. Newman, B.R. O'Keefe, S.L. Morris-Natschke, K.H. Lee, K. Nakagawa-Goto, J. Nat. Prod. 79 (2016) 2883–2889.
[22] C. Morita, Y. Kobayashi, Y. Saito, K. Miyake, H. Tokuda, N. Suzuki, E. Ichiishi, K.H. Lee, K. Nakagawa-Goto, J. Nat. Prod. 79 (2016) 2890–2897.
[23] X. Wu, L.Z. Fang, F.L. Liu, X.J. Pang, H.L. Qin, T. Zhao, L.L. Xu, D.F. Yang, X.L. Yang, RSC Adv. 7 (2017) 31115–31122.
[24] D. Xu, M.H. Luo, F.L. Liu, D. Wang, X.J. Pang, T. Zhao, L.L. Xu, X. Wu, M.Y. Xia, X.L. Yang, Sci. Rep. 7 (2017) (1964) 11956–11961.
[25] L.L. Xu, P. Hai, S.B. Zhang, J.F. Xiao, Y. Gao, B.J. Ma, H.Y. Fu, Y.M. Chen, X.L. Yang, J. Nat. Prod. 82 (2019) 221–231.
[26] A.D. Becke, Phys. Rev. A 38 (1988) 3098–3100.
[27] C. Lee, W. Yang, R.G. Parr, Phys. Rev. B 37 (1988) 785–789.
[28] D.M. York, M. Karplus, J. Phys. Chem. A 103 (1999) 11060–11079.
[29] H.D. Flack, Acta Crystallogr. Sect. A: Found. Crystallogr. 39 (1983) 876–881.
[30] F. Abas, K. Shaari, D.A. Israf, S. Syafri, Z. Zainal, N.H. Lajis, J. Food Compos. Anal. 23 (2010) 107–112.